

Validation of the NATO-standard ship signature model (SHIPIR)

D.A. Vaitekunas^{a†}, D.S. Fraedrich^{b††}

^aW.R. Davis Engineering Limited, 1260 Old Innes Road,
Ottawa, Ontario, Canada, K1B 3V3

^bNaval Research Laboratory, Code 5757,
Washington, D.C., 20375

ABSTRACT

An integrated naval infrared target, threat and countermeasure simulator (SHIPIR/NTCS) has been developed. The SHIPIR component of the model has been adopted by both NATO and the US Navy as a common tool for predicting the infrared (IR) signature of naval ships in their background. The US Navy has taken a lead role in further developing and validating SHIPIR for use in the Twenty-First Century Destroyer (DD-21) program. As a result, the US Naval Research Laboratory (NRL) has performed an in-depth validation of SHIPIR. This paper presents an overview of SHIPIR, the model validation methodology developed by NRL, and the results of the NRL validation study. The validation consists of three parts: a review of existing validation information, the design, execution, and analysis of a new panel test experiment, and the comparison of experiment with predictions from the latest version of SHIPIR (v2.5). The results show high levels of accuracy in the radiometric components of the model under clear-sky conditions, but indicate the need for more detailed measurement of solar irradiance and cloud model data for input to the heat transfer and in-band sky radiance sub-models, respectively.

Keywords: ship signature, infrared, model validation

1. INTRODUCTION

SHIPIR/NTCS^{1,2} is a model which simulates the infrared radiance of both ship targets and the maritime background (Figure 1). The model was developed by Davis Engineering and was originally funded by the Canadian Department of National Defence, through the Defence Research Establishment Valcartier (DREV). It consists of several major sub-models (Figure 2): an infrared sky radiance and propagation model (MODTRAN), a sea reflectance model, a surface geometry model which enables the modelling of complex ship geometries, a heat transfer model, a surface radiance model which accounts for multi-bounce reflections, and a plume emission model which supports the prediction of both diesel and gas turbine plume radiance profiles.



Figure 1: Typical output from SHIPIR.

Since the release of version 1.0 in 1992, the model has been continually improved. Additional sub-models for the plume, flare decoy, and missile engagement were added to version 2.0, released in 1994. To reflect this added capability, the designation was changed to SHIPIR/NTCS (Naval Threat Countermeasure Simulator). In 1994, the NATO Research Study Group 5 (RSG-5),

[†]e-mail: davidv@davis-eng.on.ca; web-site: <http://www.davis-eng.on.ca>; Tel: 613-748-5500

^{††}e-mail: fraedric@ninja.nrl.navy.mil

which specializes in IR maritime targets and backgrounds, sponsored an IR ship modelling workshop to evaluate the state-of-the art in IR ship modelling, and subsequently select a model to become the NATO Standard. After a review of many ship models, from the US and other NATO countries, SHIPIR was selected to be the NATO Standard. Based on a validation study³ performed in 1993, a series of upgrades were specified by RSG-5 and implemented. These and subsequent model improvements are summarized in Figure 3. The resulting NATO version (v2.3) was released in early 1997, and distributed to all RSG-5 countries for evaluation. During 1997/98, a number of significant improvements were made to the plume model and user interface⁴, sky model⁵, and released as version 2.4. Recent enhancements to the sea radiance model, based on the work of Mermelstein et al.⁶, were incorporated into the latest version (v2.5) and are evaluated in this paper.

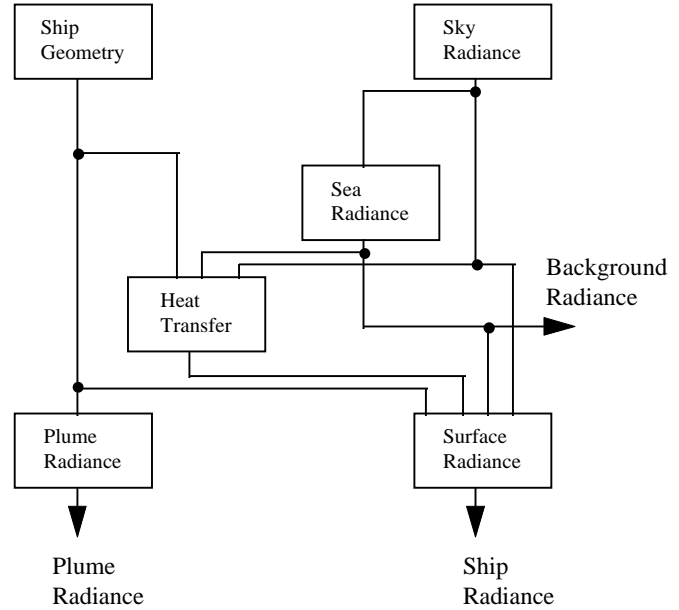


Figure 3: Block diagram illustrating sub-models of SHIPIR.

2. VALIDATION METHODOLOGY

A detailed description of the validation methodology developed by NRL to evaluate SHIPIR and other such predictive simulation codes has been reported elsewhere⁷. The basic methodology involves a four step process. Step 1 determines whether the simulation can actually be validated. The guidelines of Hodges and Dewar⁸ are used to separate simulations into predictive (i.e., those that can be validated scientifically) and non-predictive (i.e., virtual-reality training simulators which can only be evaluated using simulation-specific techniques). Step 2 is a priori evaluation which takes place before any simulation-specific experiments are conducted, to verify the model using appropriate Defence Modeling and Simulation Office (DMSO) guidelines⁹, review previous validation work on individual sub-models, and review previous validation of older versions of the aggregate system model. Step 3 is the design and execution of a new experiment, specific to the purpose of validating a particular simulation over an appropriate domain. Step 4 is the post-validation diagnosis of errors, used to either better understand the phenomenology being modelled, or further improve the prediction accuracy of the simulation.

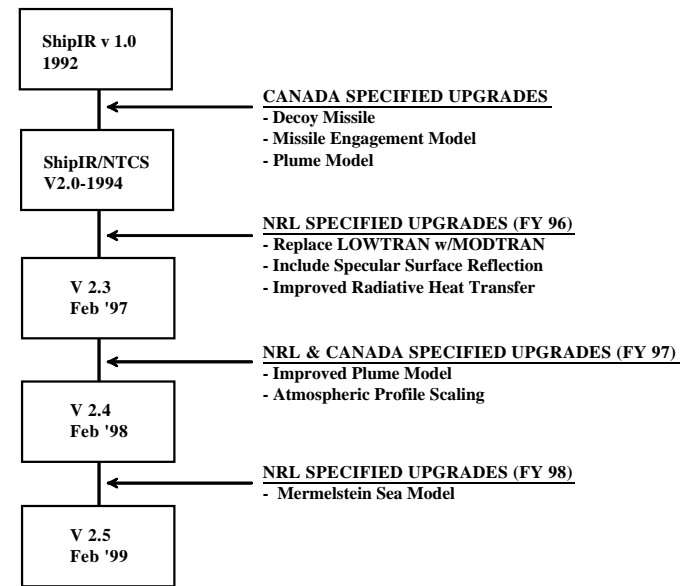


Figure 2: Evolution of SHIPIR/NTCS.

3. VALIDATION STUDY ON SHIPIR

3.1 Verification

Verification is the process of ensuring the simulation is a faithful representation of the intended underlying conceptual models. It is primarily a "debugging" task for which there are several tests available: fixed value tests and extreme condition tests⁷. Verification tends to focus on specific data and routines, and this was performed by Davis Engineering.

3.2 Review of Previous Validation Work

The only legacy sub-model used in SHIPIR is LOW/MODTRAN¹⁰. This simulation code was developed by the Air Force to predict optical propagation (transmission and path radiance) over a specified path. MODTRAN is mainly used by SHIPIR to predict the in-band radiance profile of the sky. Sky radiance subsequently affects in-band sea radiance, radiative heat transfer with the ship, and in-band reflected radiance off the ship. The most applicable validation study of MODTRAN, one which focuses on the prediction of sky radiance, is that of Wright¹¹, where measured sky radiance profiles are compared to those predicted by both MODTRAN and LOWTRAN7. The relative prediction accuracy of MODTRAN degrades with elevation, attaining a value of 20% at 60° above the horizon, and 40% at zenith (straight up). A more recent validation study using MODTRAN3 has been reported by Wang and Anderson¹².

Three previous validation studies were performed on SHIPIR, two by Davis Engineering^{3,13} and one by the Dutch Laboratory FEL-TNO¹⁴. The two by Davis Engineering used a previous NRL data set from 1992 and focussed on the facet-background radiance predictions. Both studies assessed prediction accuracy and made suggestions to improve the model. Many of the recommended improvements were incorporated into versions v2.4 and v2.5. The validation study performed by FEL-TNO compared measured total ship (contrast) radiant intensity (ship and plume) of the Dutch frigate Van Nes to predictions using version v2.3. The prediction accuracy of SHIPIR was approximately 20% for the limited runs analysed in the 8-12µm band.

3.3 Summary of Plume Model Validation

Previous work on plume model validation is treated separately since it was not part of the present validation experiment. The plume model predicts the IR radiance of an exhaust gas plume based on its exiting mass flow rate, temperature, soot density, and partial pressures of CO₂, H₂O, CO, O₂, and N₂. Three studies have been performed to date to validate the plume model in SHIPIR (v2.3): spectral validation of the individual gas band models, qualitative spectral comparison with measurement (to assess whether the correct molecules are being modelled), and band-averaged validation of the integrated plume model for maritime diesel and gas turbine engines.

3.3.1 Validation of Gas Band Models

Band models for both CO₂ and H₂O were evaluated by comparing the predicted spectral absorption values with data obtained from the Arnold Engineering Development Center (AEDC)¹⁵. Comparisons were made for gas temperatures of 300°K and 500°K, a concentration of 30 ppm, and a path length of 1 m. For CO₂ at 500°K, the predicted peak spectral absorbance (at 4.3µm) was within 20% of the measured value. Good agreement is maintained from 4.15µm to 4.45µm. In the 8-12µm band, the measured spectral absorbance has a maximum of 5×10^{-6} , and therefore CO₂ is not considered an important emitter in this band. The measured H₂O spectral absorbance remained fairly low ($< 1 \times 10^{-4}$) within the bands of interest (3.0-5.0µm and 8.0-12µm), and is therefore not considered a significant source of IR emission.

3.3.2 Full Plume Spectral Comparison

From high spectral resolution measurement of a General Electric LM2500 gas turbine¹⁶, taken by the Canadian DREV Laboratory, NRL analysed the individual emitting gas species in the plume to determine which molecular species were dominant emitters in the IR. The major plume gas constituents are¹⁷: N₂, O₂, H₂O, CO₂, Ar, NO_x, SO₂, CO, HC, and particulate carbon (soot). Of these, N₂, O₂, Ar and NO_x are known to have no emission bands in either the 3-5 or 8-12µm spectral regions. The SHIPIR plume model only considers CO₂, H₂O, CO, O₂, N₂, and soot. While both SO₂ and HC are known to emit in the 3-5µm range (3.9-4.0µm and 3.4-3.6µm, respectively), the relative importance of these emissions to the overall plume signature is not known. The spectral measurements indicate that CO₂ and CO are the major emitters in the 3-5 µm band; H₂O and HC were determined to be minor emitters (at least for the range of power settings tested). In the 3-5µm band, it was difficult to assess the relative contribution from soot emissions, since there was a significant graybody emission from stack metal exposed to the exhaust gas. There was no evidence of any SO₂ emission at 4.0µm.

3.3.3 Full Plume-Model Validation

Quantitative comparisons between ship engine plume measurements and model predictions have been made on two classes of ships: a German Type 123 Frigate¹⁸ and a Dutch M-Frigate¹⁴. In the German study, separate comparisons were made of diesel (MTU) and gas turbine (GE LM2500) plumes. The Dutch study focused only on diesel (Stork-Wartsila) plume

comparisons. Both studies compared band-average radiant intensity (3-5 μ m) measurements with SHIPIR predictions using version v2.3. The overall prediction accuracy was in the range of 20-25%, with no apparent difference in accuracy between diesel and gas turbine.

The conclusion of this plume study is as follows: 1) the major molecular emitters are being modelled, 2) the band emission models used for these major emitters are adequate in the spectral regions of high relative emission, 3) band-average radiometric comparisons with ship plumes indicate a reasonable level of accuracy (20-25%) for both diesel and gas turbine plumes. More research is required to quantify the relative contributions from soot and HC, and to determine whether the current CO band model is adequate.

3.4 Design of Validation Experiment

The objective of the model validation experiment was to 1) assess the model prediction error and 2) localize and identify any model specification errors. A number of design principles were followed in planning the experiment. Adequate measurement accuracy for both the endogenous variable (in-band radiance) and all exogenous variables (input parameters) is required to ensure the difference between measurement and prediction are only due to model specification errors, and not the result of direct measurement error, or the propagation of errors in the measured input parameters. Adequate variation of the input parameters (domain coverage) is essential to validate the model over a significant portion of its intended domain. The intermediate parameters, those internal to the model but neither input nor output of the aggregate model, can be compared with measurement (when available) to localize and identify sources of error at the aggregate level. A large number of data points (greater than the number of inputs) is required to obtain any significance in the statistical analysis of errors. Control over input variables is essential to obtain a strong correlation between a single input and output variable (i.e., when patterns do emerge in the residuals, they are unambiguously tied to one identifiable input parameter).

3.4.1 Accuracy Requirements

The goal of prediction accuracy was arbitrarily selected to be 1°C in apparent contrast temperature, corresponding to an approximate contrast radiance of 0.06W/m²·sr in the 3-5 μ m band, and 0.60 W/m²·sr in the 8-12 μ m band. To specify the accuracy requirement for each input parameter, a sensitivity analysis was performed on the model to determine the value of input error which would propagate to the specified level of accuracy in the output variable. These values along with estimated actual measurement accuracy^{19,20} are shown in Table 1. All measurement accuracies are shown to be adequate except for visibility and 3.5–4.1 μ m in-band radiance.

3.4.2 Domain

The domain of applicability for this model was determined through a statistical analysis of major weather-related input parameters over the areas-of-interest to the U.S. Navy. The domain was specified by the 5 and 95 percentile levels for each parameter obtained from weather data at NSWC-Dahlgren²¹. Average weather conditions for the Chesapeake Bay area during the month of May were obtained²² to determine if the environmental conditions for the test site were expected to fall within the defined domain. To maximize domain coverage, the test window was scheduled to last as long

Table 1: Accuracy requirements for input parameters.

Parameter	Actual Accuracy	Required Accuracy
air temperature	±0.5°C	±2°C
sea temperature	±0.5°C	±2°C
solar irradiance	±5%	±15%
cloud cover	±1/8	±2/8
wind speed	±0.5 m/s	±3 m/s
humidity	±5%	±5%
visibility	±30%	±20%
solar absorptivity	±0.05	±0.1
thermal emissivity	±0.1	±0.25
in-band reflectance	±0.05	±0.1
thermal conductivity	±10%	±50%
internal temperature	±0.5°C	±2°C
panel temperature	±0.5°C	±2°C
in-band radiance (W/m ² ·sr)		
3.5–4.1 μ m	±0.03	±0.01
4.4–5.0 μ m	±0.04	±0.03
8.2–11.8 μ m	±0.50	±0.52

as possible, within cost and programmatic constraints.

3.4.3 Intermediate Parameters and Variable Control

Several intermediate parameters were measured for the purpose of post-validation error analysis: sky radiance for the MODTRAN sky radiance sub-model, solar irradiance for the MODTRAN sun model, sea radiance for the Mermelstein sea model, and panel temperature for the heat transfer sub-model. Once prediction errors have been narrowed to the sub-model level, it is necessary to have a well-controlled experiment to yield any useful information on model specification errors. The test article was designed as an array of separate, thermally isolated test panels, each with different optical coatings, covering a range of solar absorptivity (α), thermal emissivity (ϵ), and in-band reflectance (ρ). The paints on these panels were selected to exhibit three levels of solar absorptivity (white, gray and black) and three levels of IR in-band diffuse reflectance (low, medium, and high). The optical properties for two of the six panels, UFB (Flat-black) and white, are shown in Table 2. Other important variables are the cloud cover and solar irradiance. Since the sky model does not account for fractional cloud cover, data were only collected under clear-sky and completely overcast conditions. Adequate variation in solar irradiance was obtained by collecting data at different times of the day and night.

Table 2: optical properties for two of the test panels.

Parameter	UFB	White
α (solar)	0.94	0.25
ϵ (thermal)	0.95	0.90
ρ (3–4 μm)	0.04	0.18
ρ (4–5 μm)	0.04	0.32
ρ (8–12 μm)	0.05	0.08

3.4.4 Number of Data Points

For SHIPIR, there are approximately 20 input parameters per panel per spectral band. To achieve a reasonable number of statistical degrees of freedom (>10), at least 30 data points are needed per band. With six panels, at least five runs are required. Further details on the test plan can be found in the Test Plan²³.



Figure 4: Test article on LCM craft.

3.5 Execution of Experiment

Measurements were made on 5 different days during a 4-week period from 12 May to 5 June 1998 at NRL's Chesapeake Bay Detachment. The 6-panel test article was installed on the NRL LCM 8 craft (Figure 4), along with a weather station and thermocouple (panel temperature) measurement system. Data were collected for a total of 20 runs, with runs 1 through 4 on 14 May used as "dry runs" for instrument calibration and adjustment. Runs 17 and 18 were aborted due to broken cloud cover. The resulting weather parameters for the 14 remaining runs are shown in Table 3. The range of parameters are compared with the required domain in Table 4. All measurements were taken within the specified range, but they did not cover the entire domain. The sea temperature was in the middle of the range, the air-sea temperature difference in the top one-third, and the wind speed only in the bottom one-fifth. Future validation experiments should cover the remainder of the domain.

3.6 Analysis of Experiment

3.6.1 Predicted Temperature

The contrast temperature predictions for the UFB and white panels, plotted against those measured, are shown in Figure 5, with the associated error statistics shown in Table 5. The predicted panel temperatures are consistently lower than the measurement, and this was true for all panels. A majority of the runs were executed under clear and overcast daytime conditions. Since SHIPIR currently performs only steady-state heat transfer calculations, the first step in assessing these errors was to plot the results against the measured temporal derivative in each panel temperature (dT/dt), as shown in Figure 6. These results show

Table 3: Experimental data set.

Run	Date	Time	T _{air} (°C)	T _{sea} (°C)	Cloud (%)	Wind (m/s)	RH (%)	Vis. (nm)	Solar (W/m ²)
5	135	10:20	17.3	17.4	0	1.5	69	>15	500
6	135	12:10	17.7	17.6	0	1.4	69	>15	500
7	135	14:10	19.7	17.8	0	2.7	75	>15	300
8	135	16:10	20.3	17.4	0	2.6	78	>15	80
9	138	09:50	20.9	20.3	0	2.3	67	>15	450
10	138	12:00	23.5	21.6	0	2.2	59	>15	500
11	138	14:00	25.5	21.4	0	1.2	46	>15	260
12	139	20:30	25.7	21.1	0	1.7	59	12	0
13	139	22:20	25.1	20.5	0	2.7	58	12	0
14	147	10:20	20.1	20.5	100	2.2	80	10	100
15	147	12:20	22.2	20.5	100	1.3	73	7	270
16	147	14:25	21.1	20.9	100	0.7	78	5	130
19	155	21:50	21.3	22.2	100	1.9	71	8	0
20	155	23:30	21.1	21.9	100	3.1	71	>15	0

Table 4: Comparison of actual and required domain coverage.

Parameter	Actual Range	Required Range
sea temperature	17 – 23°C	7 – 34°C
air-sea temperature difference	-0.8 – 4.6°C	-9 – 5°C
solar condition	day & night	day & night
cloud cover	0 and 8/8	0 and 8/8
wind speed	0.7 – 3.0 m/s	1 – 15 m/s
humidity	45 – 80 %	15 – 98 %
visibility	8 – 25 km	2 – 50 km
panel solar absorptance	0.25 – 0.94	0 – 1
panel thermal emissivity	0.05 – 0.95	0 – 1
panel IR reflectance	0.04 – 0.95	0 – 1

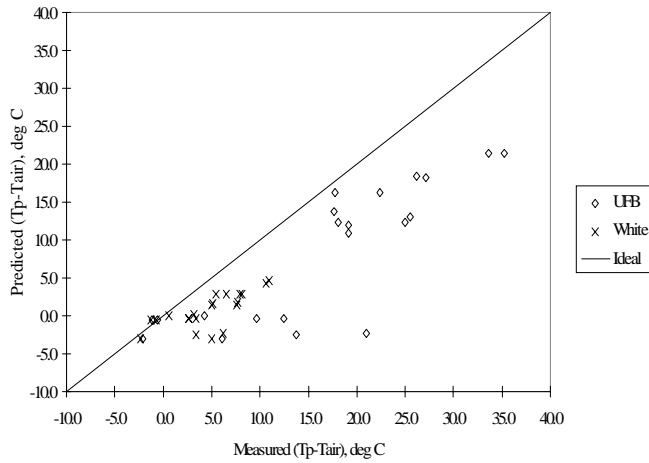


Figure 5: Predicted panel contrast temperatures.

Table 5: Panel contrast temperature statistics

Errors (°C)	UFB	White	All
avg.	-8.4	-4.0	-5.2
max. abs.	23.3	8.6	23.8
RMS	10.2	4.7	7.8

the correct trend in temperature: under-prediction at high $-dT/dt$ and over-prediction at high $+dT/dt$ are expected when the low or high temperatures, respectively, have not been achieved yet. The next step looked at the data near thermal equilibrium ($|dT/dt| < 0.15^\circ\text{C}/\text{min}$) and searched for a correlation with any intermediate variables. By comparing the predicted solar irradiance (E_{sun}) incident on the panels with that measured by the pyranometer (0.4–1.1 μm band), taking into account the solar absorptivity of each panel, the results in Figure 7 were obtained. A large majority of the errors are directly correlated with errors in predicted solar irradiance. Work is currently underway to assess the sensitivity of solar irradiance to both visibility and target heading. The remaining data, with little or no sun present, were assessed to determine the degree to which convection may have influenced the temperature error. The following convection factor was defined:

$$K_{\text{conv}} = \frac{U_{\text{air}}(T_p - T_{\text{air}})}{\varepsilon_T [E_b(T_p) - E_{\text{bck}}(\theta_p)]} \quad (1)$$

relating the convective heat transfer to and radiative heat transfer. Forced (wind-driven) convection is proportional to wind speed and panel contrast temperature, while radiative heat transfer is proportional to the emissivity and thermal irradiance contrast between panel and background. Without

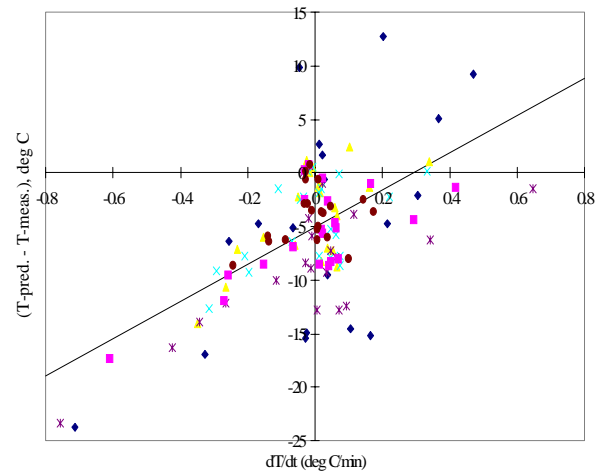


Figure 6: Effect of non-thermal equilibrium on temperature prediction.

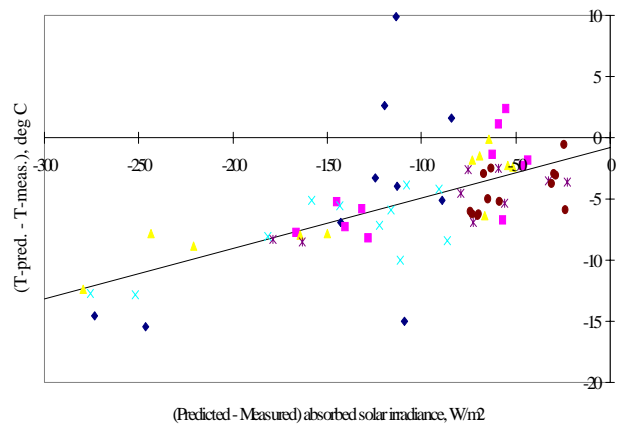


Figure 7: Effect of solar irradiance prediction error.

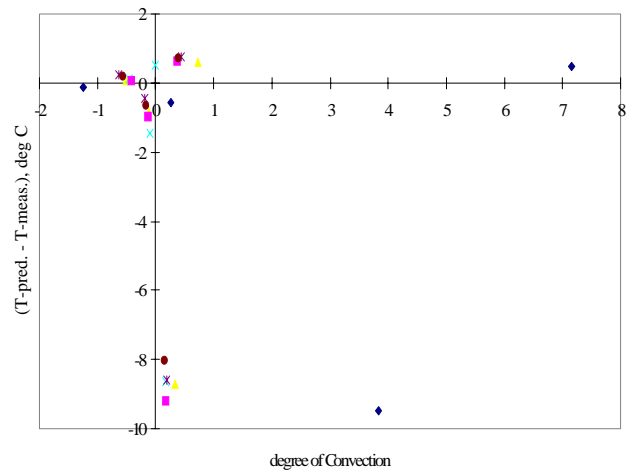


Figure 8: Sensitivity of panel temperature (no-sun) to convection.

the sun, the panels achieve a thermal equilibrium where convective heat transfer exactly equals radiative heat transfer (equal and opposite). Highest values of K_{conv} (see Figure 8) indicate data points where convection had the strongest effect. The non-sensitivity of panel temperature error to this convection factor further indicates a dominance by prediction errors in solar irradiance. The very large under-prediction in Figure 8 was obtained from run 12 (executed just after sunset), where one can assume an appreciable amount of solar scattering remains unaccounted for by both the model and pyranometer.

3.6.2 Predicted Radiance

Figure 9 shows the predicted radiance for both the UFB and white panels (based on measured panel temperature), and the sea background 1 degree below the horizon. The corresponding statistical analysis results are provided in Table 6, along with those for the predicted panel radiance based on predicted temperature. The contrast temperature (ΔT_{app}) corresponding to each RMS error indicates to what extent the original goal of 1 °C was met. The results indicate the error in predicted radiance is somewhat larger than the measurement error, even when the panels are set to the measured temperature. Further analysis resulted in the curves presented in Figure 10, where the error in panel radiance is compared to the accuracy of the method used to approximate the spectral response curve of the imaging radiometers^{19,20}. The present method uses a 1/2-power approximation, where the normalized spectral response of the radiometer is approximated by an equivalent unit step-response between two specified wavelengths (e.g., 4.4–5.0 μm). Detailed analysis of the actual spectral response of the two radiometers shows a high degree of correlation between the error in predicted radiance and the error in this approximation. The UFB panel was used in this assessment, since it has very little or no background reflection. SHIPIR (v2.5) now includes an option to input and model the detailed spectral response of the imager. Further analysis of the other band-average assumptions used in the radiance model (band-average reflectance, band-average multi-bounce diffuse-radiosity), and thermal model (thermal emissivity and solar absorptivity) is required to assess their similar effect on overall prediction accuracy.

Table 6: Panel and sea radiance statistical error analysis

Errors (W/m ² ·sr)	Predicted-Temperature			Measured-Temperature			Sea
	UFB	White	All†	UFB	White	All†	
SWF1: 4.4-5.0 μm							
avg.	-0.241	-0.041	-0.066	0.059	0.035	0.022	0.039
max. abs.	0.753	0.187	0.753	0.204	0.113	0.204	0.130
RMS	0.348	0.079	0.167	0.076	0.053	0.070	0.075
ΔT_{app} (°C)	±10	±2.5	±5.1	±2.4	±1.7	±2.2	±2.4
SWF2: 3.5-4.1 μm							
avg.	-0.067	0.013	0.013	0.055	0.047	0.051	0.028
max. abs.	0.183	0.062	0.239	0.089	0.078	0.265	0.070
RMS	0.100	0.031	0.069	0.058	0.053	0.071	0.041
ΔT_{app} (°C)	±9.2	±3.2	±6.7	±5.7	±5.3	±7.0	±4.1
LW: 8.2-11.8 μm							
avg.	-2.96	-0.81	-0.90	1.285	0.925	0.772	1.069
max. abs.	11.38	3.82	11.38	3.78	3.19	4.27	3.02
RMS	4.62	1.59	2.84	1.47	1.16	1.59	1.80
ΔT_{app} (°C)	±9.3	±3.2	±5.7	±3.0	±2.4	±3.3	±3.7

† includes all six panels and sea radiance

Background radiance profiles were also measured and compared with SHIPIR, as shown in Figures 10 and 11 for the clear-sky and cloudy-sky daytime runs, respectively. The results show very good agreement for the clear-sky conditions, both day and night. An improvement made to the sky model (v2.4) allows the local measurement of air temperature and relative humidity to be used to scale the internal atmosphere profiles of both LOWTRAN and MODTRAN to fit the sea-level values. For overcast conditions, the default cumulus cloud model was arbitrarily chosen (base=0.66 km, thickness=2.34 km), and the resultant flat over-prediction of sky-radiance indicates this to be incorrect. Subsequent cloud measurements, obtained 30 miles south of the test site on 27 May (base=2.4 km) and 4 June (base=1.2 km), suggest a higher-altitude cumulus or altostratus cloud cover. The cloud thickness may be adjusted to obtain the measured in-band sky radiance profile. Work is currently underway to assess the impact of inputting measured air-temperature and relative humidity profiles, also obtained more recently.

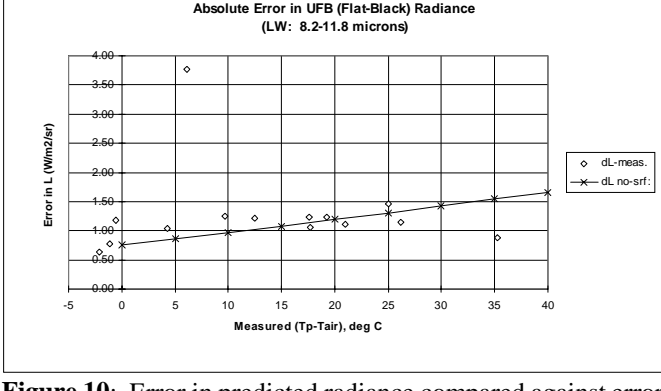
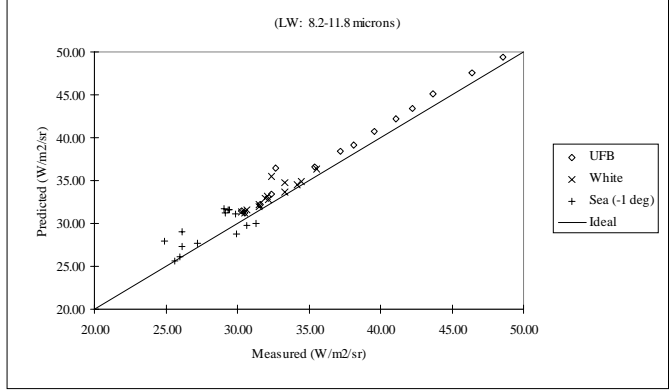
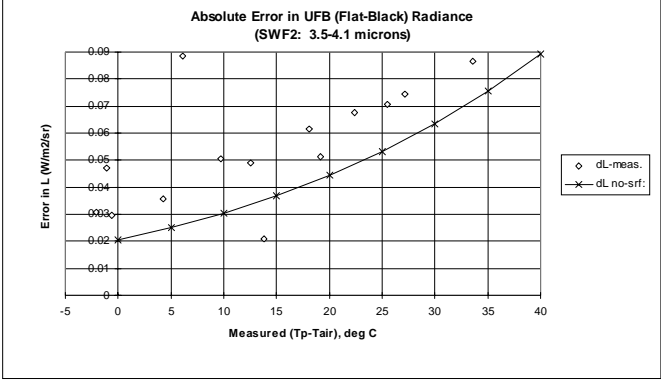
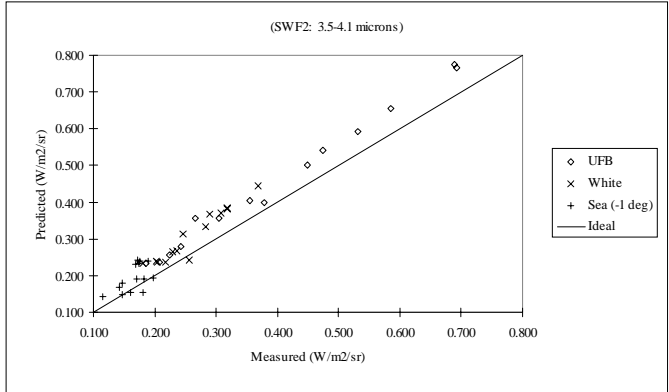
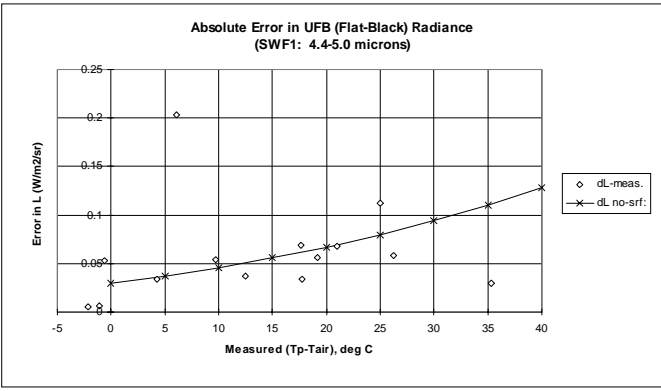
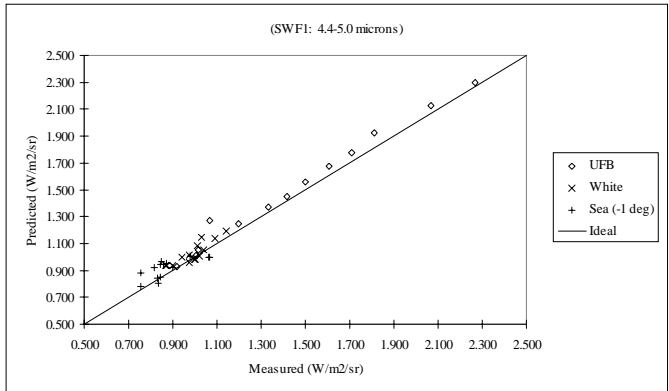


Figure 9: Predicted in-band radiance.

Figure 10: Error in predicted radiance compared against error in the approximation of spectral response.

4. SUMMARY AND CONCLUSIONS

A validation study was performed to assess the predictive accuracy of SHIPIR (v2.5). The measured data from a recent NRL panel test experiment were used to statistically compare predictions of surface temperature, in-band panel radiance, and background (sea/sky) radiance. A detailed functional analysis of the panel temperature errors (RMS of $\pm 8^\circ\text{C}$) revealed a majority are caused by thermal transients (not modelled) and mis-prediction of solar incident irradiance. It should be noted that modelling the marine target's environment as steady-state results in a worst-case scenario of daytime signature. However, there is a significant variation in ship signature, resulting from either quick changes in relative solar position (i.e., ship heading) or natural diurnal variations in the solar irradiance, which must be addressed. The thermal transients measured during the test have a strong influence on signature, and this will become more important as modern stealth warship designs²⁴ are considered. The errors in predicted radiance (RMS of $\pm 1.7\text{--}7.0^\circ\text{C}$ apparent contrast) for both the panels and the background were shown to be dominated

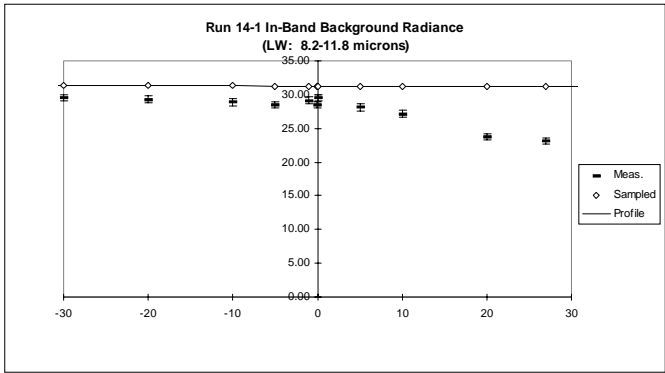
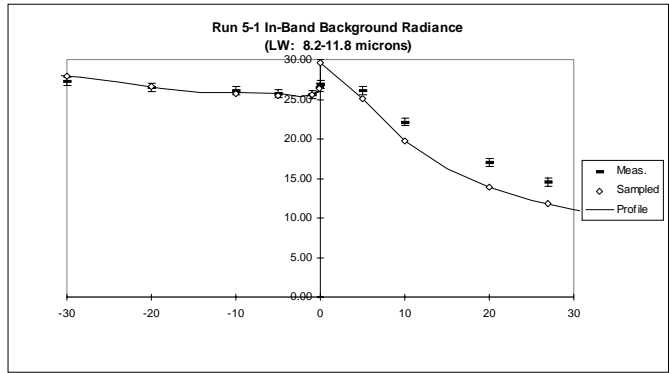
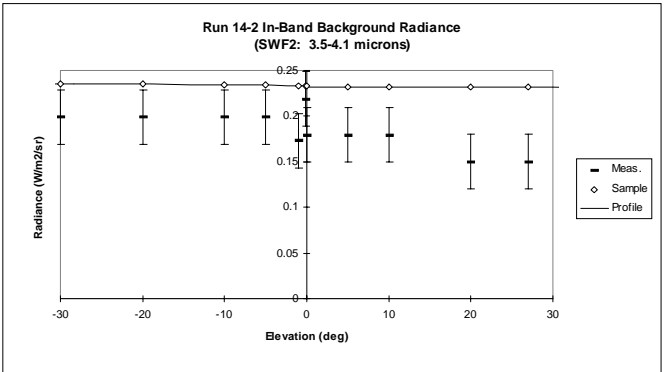
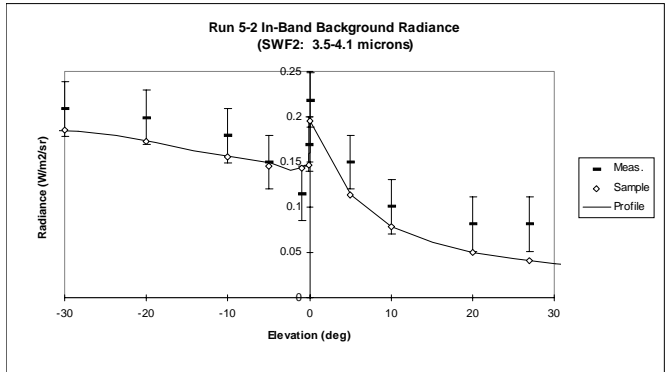
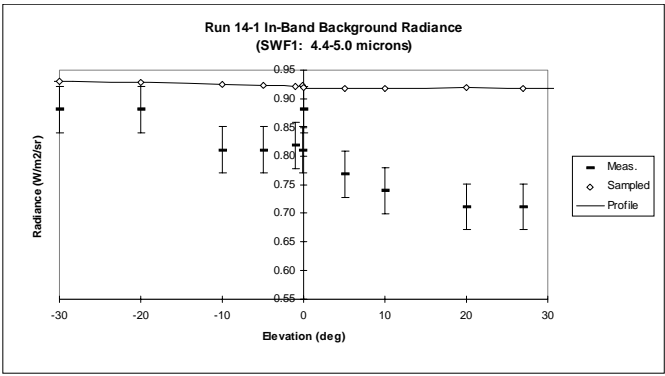
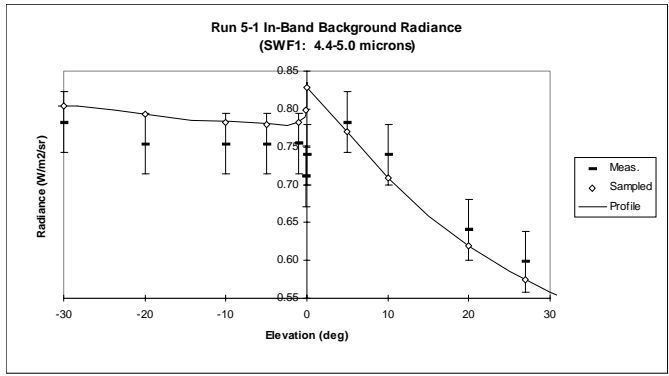


Figure 11: Background radiance profiles about the horizon on 15 May, 10:20 AM.

Figure 12: Background radiance profiles about the horizon on 27 May, 10:20 AM.

by errors in predicted temperature, sky radiance, and the use of a 1/2-power approximation for the spectral response of the radiometer. Other secondary properties such as reflected in-band irradiance and spectral material properties could not be evaluated until these other errors have been eliminated.

ACKNOWLEDGEMENTS

This work was funded by the U.S. Navy. Re-assessment of the model using the more recent version of SHIPIR (v2.5) was funded by the Canadian Department of National Defence, through the DREV Laboratory (PWGSC W7701-8-3517). The authors wish to thank both Tom Taczak of Envisioneering and Brett Brooking of Davis Engineering for their assistance in processing the model runs of SHIPIR for this validation study.

REFERENCES

1. J. Morin, F. Reid and D. Vaitekunas, "SHIPIR: a model for simulating infrared images of ships at sea," *SPIE* **2223**, 1994.
2. D.A. Vaitekunas, K. Alexan, O.E. Lawrence, and F. Reid, "SHIPIR/NTCS: a naval ship infrared signature countermeasure and threat engagement simulator," *SPIE* **2744**, pp. 411-424, 1996.
3. D.A. Vaitekunas and K. Alexan, "SHIPIR Validation for RSG-5," Davis Engineering Technical Report (File #A301), November 1993.
4. "Release Notes: the NATO-Standard Ship Signature Code NTCS (v2.4)," Davis Engineering Technical Report (File #A703), March 1998.
5. "Improvements to the Sky Model of the NATO-Standard Ship Signature Code (v2.4)," Davis Engineering Technical Report (File #A801), February 1998.
6. M.D. Mermelstein, E.P. Shettle, E.H. Takken, and R.G. Priest, "Infrared radiance and solar glint at the ocean-sky horizon," *Appl. Opt.* **33** (25), pp. 6022-6034, 1994.
7. D. Fraedrich and A. Goldberg, "A Methodological Framework for the Validation of Predictive Simulations," To be published European Journal for Operational Research 1998.
8. J. Hodges and J. Dewar, "Is it you or your model talking? A Framework for Model Validation," Rand Nomograph R-4114-AF/A/OSD 1992.
9. "Verification, Validation and Accreditation (VV&A) Recommended Practices Guide," Office of the Director of Defence Research and Engineering, Defence Modeling and Simulation Office, November 1996 (See <http://www.dmsi.mil/docslib/mspolicy/vva/rpg>).
10. A. Berk, L.S. Bernstein, and D.C. Robertson, "MODTRAN: A Moderate Resolution Model for LOWTRAN 7," AFGL-TR-89-0122, 1989.
11. J. Wright, "Accuracy of LOWTRAN 7 and MODTRAN in the 2.0-5.5 μm Region," *Appl. Opt.* **33**, p. 1755, 1994.
12. J. Wang, G.P. Anderson, H.E. Revercomb, and R.O. Knuteson, "Validation of FASCOD3 and MODTRAN3: comparison of model calculations with ground-based and airborne interferometer observations under clear-sky conditions," *Appl. Opt.* **35** (30), pp. 6028-6040, 1996.
13. "Validation of the NATO-Standard Ship Signature Model (NTCS) Using NRL Panel Data" Davis Engineering Technical Report (File #A707), September 1997.
14. F. de Groote, "Vergelijking van ShipIR (v2.3) simulaties aan het M-fregat met metingen uit het rapport FEL-91-A034", FEL-TNO Technical Report (In Dutch), September 1997.
15. "SHIPIR/NTCS Training", Course Handouts, Davis Engineering, 1998.
16. "Canadian IR Spectral Imagery Presentation" Presentation given by T. Smithson at the NATO ShipIR Workshop, 27 May, 1998.
17. Manufacturer data forwarded by Mike Osborne, NAVSEA 03Z, May 1998.
18. "ShipIR Results in Comparison" Presentation given by M. Janssen at the NATO ShipIR Workshop, 27 May, 1998.
19. D. Fraedrich, "Methods in Calibration and Error Analysis for Infrared Imaging Radiometers," *Opt. Eng.*, **30**, p. 1764, 1991.
20. R. Patchan, "Absolute Radiometric Techniques and Error Analysis for Imaging Radiometers in a Field Environment," *SPIE*, **2470**, p. 224, 1995.
21. "NSWC-Dahlgren R756 Littoral Database" (See <http://www.nswc.navy.mil>).
22. "U.S. Navy Marine Climatic Atlas of the World, Version 1.1" Navy Meteorological and Oceanography Command, 1995.
23. "Test Plan for Panel Test '98," NRL Internal Document, April 1998.
24. J. Thompson, D. Vaitekunas, and A.M. Birk, "IR Signature Suppression of Modern Naval Ships", Presented at *ASNE 21st Century Combatant Technology Symposium*, 27-30 January 1998.